Transactions, SMiRT-24
BEXCO, Busan, Korea - August 20–25, 2017
Division VI (include assigned division number from I to X)

APPLICABILITY EVALUATION OF STEEL PLATE REINFORCED CONCRETE STRUCTURE TO PRIMARY CONTAINMENT VESSEL OF BWRS
(12) PRESSURE TEST OF CYLINDRICAL STEEL PLATE REINFORCED CONCRETE STRUCTURE

Junya Kawada,[1] Takashi Okayasu,[2] Shintaro Narita,[3] Masaaki Osaka,[4] Hideo Hirai,[5] Tetsuo Abiru[6]

[1] Engineer, Kajima Corporation, Japan
[2] Senior Research Engineer, Kajima Corporation, Japan
[3] Staff Engineer, Hitachi-GE Nuclear Energy, Ltd., Japan
[4] Chief Project manager, Hitachi-GE Nuclear Energy, Ltd., Japan
[5] Senior Specialist, Toshiba Corporation, Japan
[6] Manager, The Chugoku Electric Power Co., Inc., Japan

ABSTRACT

In order to evaluate the structural integrity of a steel plate concrete containment vessel (SCCV) for pressure loading under accident conditions, the pressure test of a cylindrical steel-plate reinforced-concrete (SC) specimen and its simulation analyses are conducted. A large scale cylindrical SC specimen (120 mm wall thickness, 2580 mm inner diameter and 1770 mm height) simulating the shell wall of the assumed actual real SCCV is fabricated. The specimen has two large openings in the lower part of the wall and a constrained slab plate at the middle height of the wall. Water pressure is applied to the inner side of the specimen until the specimen reaches the nearly maximum failure state. In this paper, the outline of the test, the results of the test, and the analyses are presented.

INTRODUCTION

In order to show that the steel plate concrete containment vessel (SCCV) can be designed with sufficient margin against pressure loads in a severe accident (SA), it is necessary to evaluate the failure mode of SCCV against the pressure load and to improve the accuracy of the analytical evaluation up to the ultimate state. Although there were several pressure tests targeting the reinforced concrete containment vessel (RCCV) [1]-[5] and the pre-stressed concrete containment vessel (PCCV) [6], no pressure test for SCCV has been conducted so far. Therefore, in this study, the pressure test using a large-scale cylindrical SC specimen simulating the assumed actual SCCV is performed, and its simulation analyses are conducted.

EXPERIMENTAL DETAILS

Outline of the test and specimen

Figure 1 shows the load conditions at the time of SA assumed for the actual SCCV. In this test, the outer shell wall is considered since it constitutes the leakage boundary of the containment vessel, and the differential pressure is more severe than the inner shell wall. A pressure test with a cylindrical SC specimen having access tunnel openings and considering the constraining effect by the diaphragm floor /

peripheral floor is conducted in order to grasp the behavior of the SC structure shell wall against the pressure load.

The specimen is a cylindrical SC specimen with a scale of approximately 1/17, the inner diameter of the cylindrical wall is 2580 mm, the internal height is 1770 mm, and the wall thickness is 120 mm. The thickness of the inner and outer surface steel plate is 1.2 mm. Shear connectors (stud: 2.53 mm in diameter, 19.2 mm in length, 24 mm in spacing) are welded on the steel plate to connect the steel plate and concrete. The ratio of the stud interval to the steel plate thickness is set to 20 so as not to cause elastic buckling until steel plate yielding. Vertical rib plates (thickness: 1.2 mm, interval: 22.5°) are placed inside the cylindrical wall, and a restraint slab plate that approximately simulates the restraining effect of the diaphragm floor and the peripheral floor at the same height in the assumed actual SCCV is installed. Openings simulating the two access tunnel openings are considered. According to JSME S NC 1 - 2008 [7], the reinforcement method around the opening is to double the thickness of the steel plate in the range of half of the opening diameter. Around the boundary part between the reinforcement area and non-reinforcement area (general area), a taper of approximately 1/3 is provided to avoid stress concentration. Two types of reinforcements—circular shape reinforcement and the rectangular shape reinforcement—are considered. Figure 2 and Figure 3 show the shapes of the specimen and opening reinforcements, respectively.

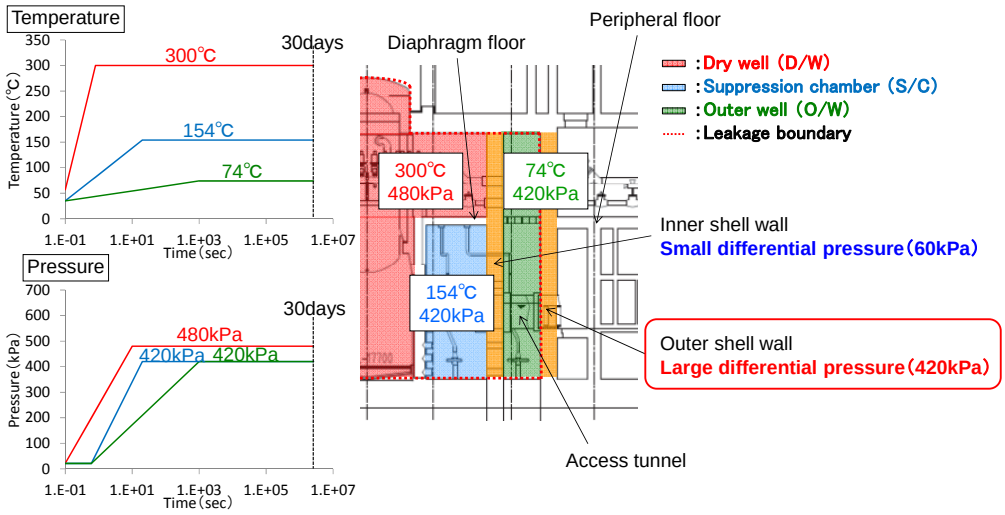

Figure 1 The load condition of SA assumed for actual plant

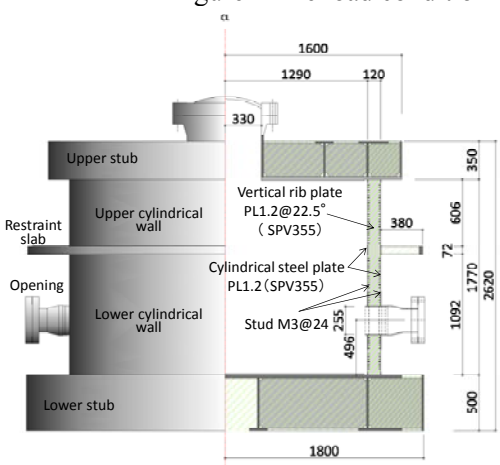

Figure 2 Shape of specimen

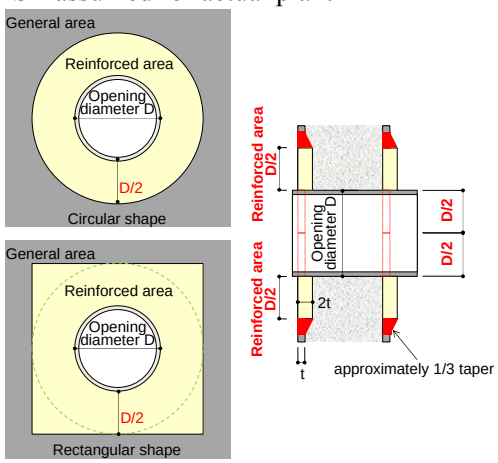

Figure 3 Shape of opening reinforcements

SPV 355 (JIS G 3115 [8]) with almost the same characteristics as the standard strength of SPV 490 (JIS G 3115 [8]), which is the candidate material of the assumed actual SCCV, is used for the steel plate. Table 1 shows the material test results of the steel plate. Table 2 shows the material test results of the concrete used for the cylindrical wall. Carbon steel with a yield strength of 375 N/mm^2 or more is used for the stud.

Table 1 Material properties of steel plate; SPV355 (t = 1.2 mm)

Static modulus of elasticity [× 10^3 N/mm^2]	Yield strength [N/mm^2]	Tensile strength [N/mm^2]
210–211	455–461	572–583

Table 2 Material properties of cylindrical wall concrete

Compressive strength [N/mm^2]	Splitting tensile strength [N/mm^2]	Static modulus of elasticity [× 10^3 N/mm^2]
48.1	3.26	3.00

Test procedures and loading apparatus

The test procedure is shown in Figure 4. The interior of the specimen is filled with water and the internal pressure is given by hydro pressure. One accident pressure, P_{SA}, indicates the maximum pressure (0.42 MPa) that the outer shell of the assumed actual SCCV receives at SA. Based on this value, the pressure is gradually increased by 0.5 × P_{SA} increments until the ultimate state.

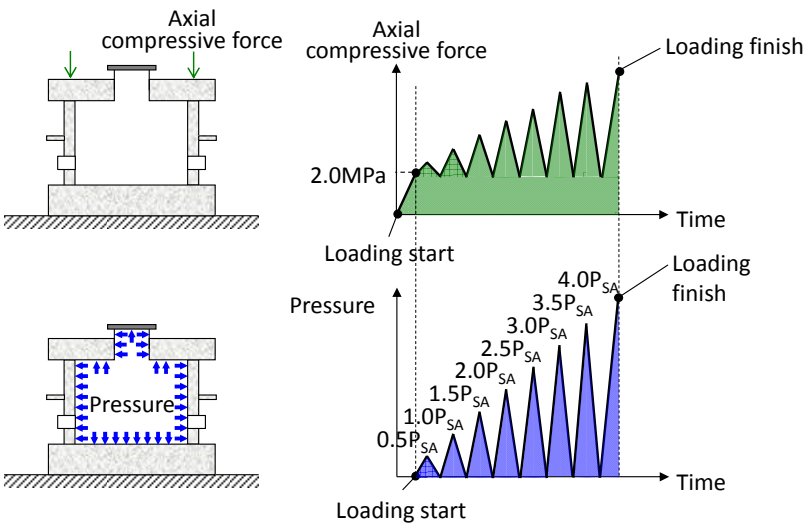

Figure 4 Test procedures

Axial compressive force of approximately 2.0 MPa as the average of all cylindrical wall cross sections is applied by hydraulic center hole jacks to simulate the axial force due to its own weight and live load. During the pressure test, the specimen receives excessive vertical tensile force compared to the axial force expected in the assumed actual SCCV caused by not simulating the inner shell wall, and additional compressive force is given according to the internal pressure so that the vertical axial stress of the specimen is equivalent to the real accident condition. Vertical compressive force is applied to the specimen by introducing tensile force to the PC steel rods with a hydraulic jack. Figure 5 shows the vertical sectional view of the axial force introduction jig and the experimental situation after installing the jig.

In addition to the internal pressure and vertical compressive force, a temperature load (74°C) is considered in the event of an accident. This test is carried out at room temperature (approximately 20°C) because the influence of the temperature on the evaluation of the failure mode of the outer shell wall is small based on the result of the preliminary analysis.

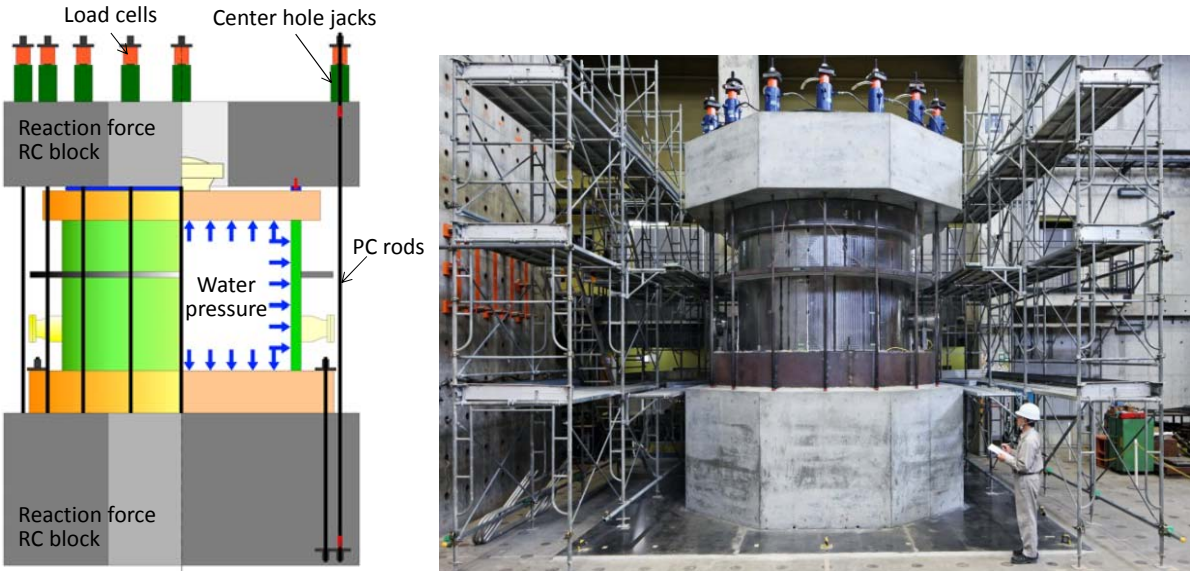

Figure 5 Axial force introduction jig and the experimental situation after installing the jig

EXPERIMENTAL RESULTS

The test was terminated after the tensile strain of the inner steel plate at the position of the base reached a large value exceeding 40000 μ. The pressure at that time was 1.70 MPa, exceeding 4 P_{SA} (1.68 MPa).
Figure 6 shows the relationship between internal pressure and transverse deformation of the lower cylindrical wall. The maximum transverse deformation of the lower cylindrical wall is at the maximum of approximately 7.4 mm on the 0° side (circular reinforcement) and at the maximum of approximately 6.6 mm on the 180° side (rectangular reinforcement). The reason why the deformation of the rectangular reinforcement side is smaller is the fact that the reinforcement area around the opening is wider than the circular reinforcement. On the other hand, the maximum transverse deformation, approximately 7.9 mm, at 90° and 270° with no opening, is almost similar. Figure 6 (b) also shows the yielding process of the steel plate. The yielding of the steel plate is determined based on Von Mises at the plane stress field. Steel plate yielding starts at 2 P_{SA} (0.84 MPa) where the thickness of the steel plate around the circular reinforcement part of the inner steel plate changes, and then the base of the inner steel plate yields from bending tension. At approximately 2.5 P_{SA} (1.05 MPa), the thick area around the opening of the outer steel plate and the thickness switching area of the inner steel plate yield almost at the same time. Thereafter, the inner steel plate of the lower cylindrical wall in the circumferential direction, the inner steel plate of the upper wall in the vertical direction, and the outer steel plate of the lower wall in the circumferential direction yield. The reason why the gradient of the internal pressure-transverse deformation relationship becomes loose from around 3 P_{SA} (1.26 MPa) is roughly coincident with the starting point of the steel plate yielding of the lower cylindrical wall.

Figure 7 shows the vertical cross-sectional distribution of the transverse deformation. Since the transverse deformation is restrained by the restraint slab at a height of 1000 mm, the largest deformation

is observed at the lower cylindrical wall. As shown in Figure 6, the deformation is greatly extended beyond 1.47 MPa. This is probably because the yielding of the entire steel plate at the lower cylindrical wall occurs from around this pressure.

Figure 8 shows the vertical cross-sectional distribution of the circumferential and the vertical strains of the general part (the position without the opening) at maximum pressure (1.70 MPa). The circumferential strain shows a large tensile strain in both the inner and outer steel plates in the lower cylindrical wall, and it is approximately 25,000 μ at maximum at 1.70 MPa. The large vertical strain is mainly generated by the bending force. The maximum tensile strain of approximately 40,000 μ occurs at the base of the inner steel plate of the lower cylindrical wall, and the compressive and tensile strain of approximately 15,000 μ occurs at the middle part of the lower cylindrical wall.

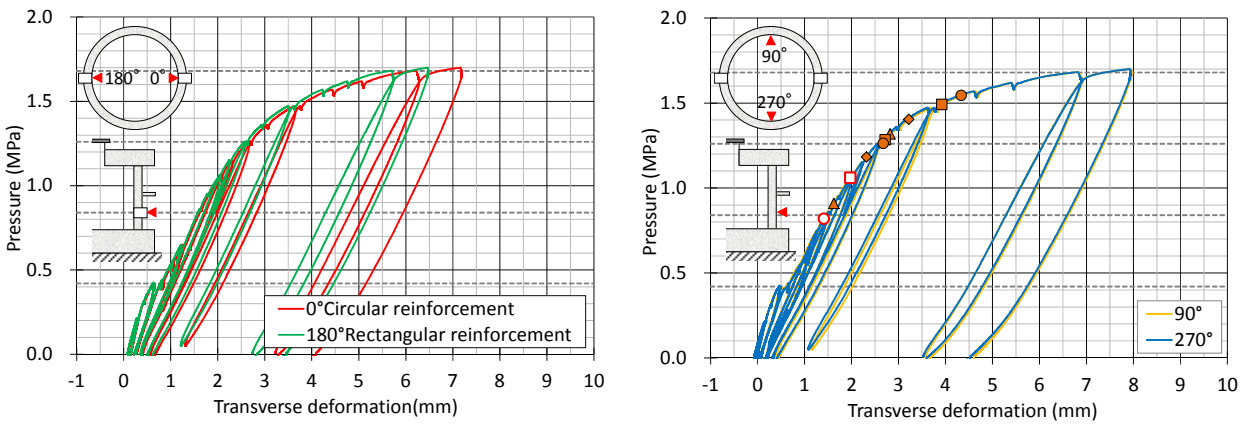

Figure 6 Relationship between internal pressure and transverse deformation of the lower cylindrical wall

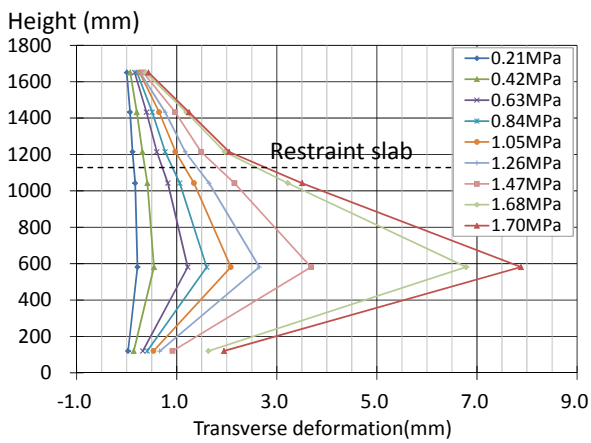

Figure 7 Vertical cross-sectional distribution of transverse deformation

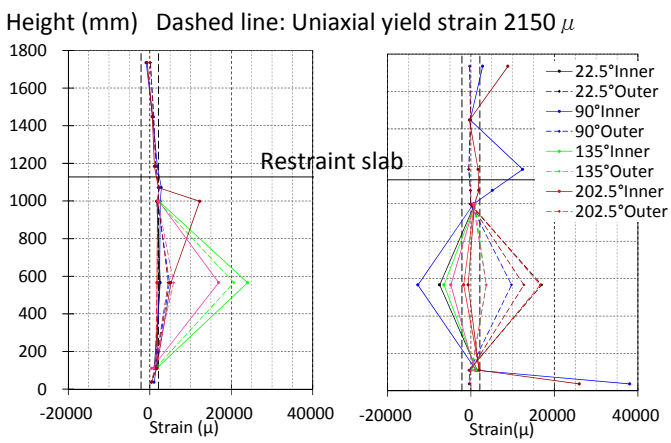

(a) Circumferential direction (b) Vertical direction

Figure 8 Vertical cross-sectional distribution of the strains

Figure 9 shows the principal strain distribution around the opening of the inner steel plate at maximum pressure (1.70 MPa). In both circular reinforcement and rectangular reinforcement, tensile yielding at the thickened part just above the opening occurs, but the value is small (① in the figure). The large strain exceeding 20,000 μ is observed at the switching part of the reinforced steel plate thickness (② in the figure). This strain is equivalent to the circumferential strain of the general part without the opening as

shown in Figure 8. Because it is confirmed that the extension of the strain around the opening is restrained, it can be said that the opening reinforcement effectively functions.

Figure 10 shows the pressure-circumferential strain relationship of the inner steel plate of the lower cylindrical wall and the pressure-vertical strain relationship at the base position of the inner steel plate. The circumferential strain around the reinforced area and the general area is approximately 25,000 μ at 1.70 MPa, respectively, which shows that the yielding area extends over the entire lower cylindrical wall. Since the vertical strain at the base part of the inner steel plate shows a sharp increase around 1.70 MPa, it can be considered that the specimen has reached the pressure limit of approximately 1.70 MPa.

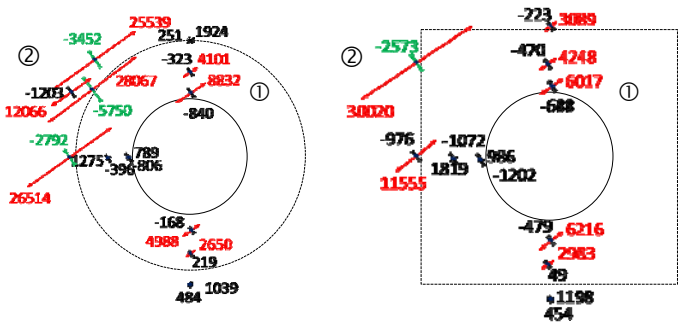

(a) Circular reinforcement (b) Rectangular reinforcement

Figure 9 Principal strain distribution around the opening of the inner steel plate (1.70 MPa)

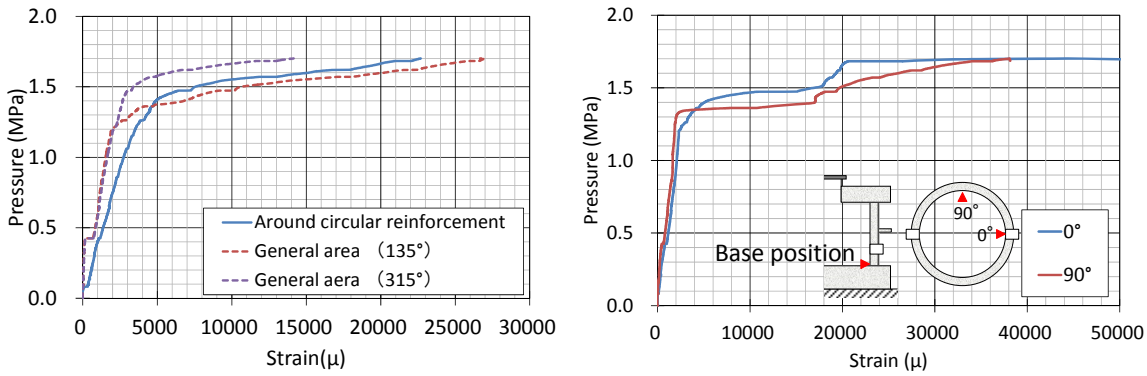

(a) Circumferential strain (b) Vertical strain at the base position

Figure 10 Pressure- strain relationship (inner steel plate)

After the test, the specimen is visually inspected, and bubble leak testing (JIS Z 2329 [9]) for the inner steel plate is carried out on the base part and the opening part where the strain is large. In either case, no damage, such as deformation or cracking due to buckling of the steel sheet, is confirmed. In addition, the specimen is cut in the vertical direction and the horizontal direction, and the state of the concrete damage is inspected. Photographs after cutting are shown in Figure 11 and Figure 12. Horizontal cracks due to bending are observed on the outer side of the center height of the lower cylinder wall, and horizontal cracks due to bending are observed at the base. Diagonal cracks due to transverse shear force are also observed on the 0° side base. However, there is no compressive crushing of the concrete and significant slippage of the cracked surface, which shows compressive bending failure or transverse shear failure of the concrete. Radial cracks generated by the circumferential force from the internal pressure are confirmed in the horizontal section.

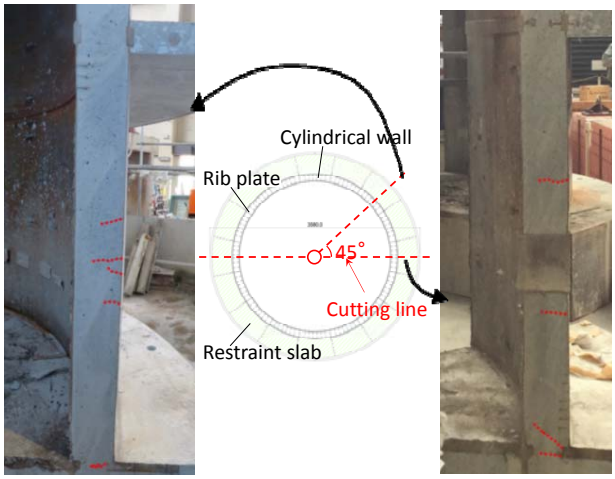

Figure 11 Vertical cutting face

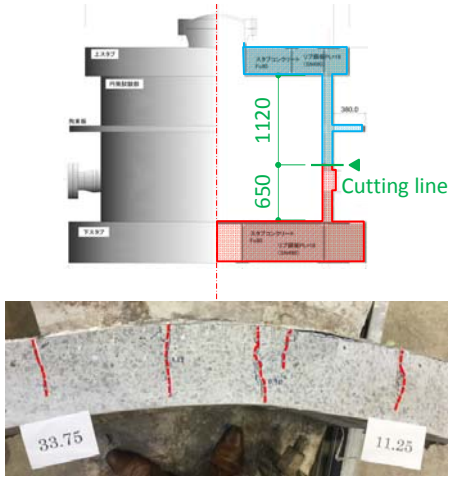

Figure 12 Horizontal cutting face (11.25°～33.75°)

The above test results can be summarized as below. In the state where maximum pressure (1.70 MPa: corresponding to approximately 4 times the pressure at SA) is applied, the steel plate of the lower cylinder wall yields over the entire area, and the maximum strain reaches up to approximately 40,000 μ. In addition, judging from the degree of strain extension, the pressure is considered to have reached a level at which the specimen cannot withstand any further load increment. From the visual inspection and the foam leakage inspection after the test, damage, such as cracks, is not observed on the steel plate and crushing of the concrete and significant slippage of the diagonal cracked surface are not observed. Judging from the above results, the final failure mode may be bending failure due to the tensile fracture of the inner steel plate at the base.

ANALYTICAL DETAILS

The model used for the simulation analysis is a 90° cutout model in consideration of the symmetry of the test specimen. In order to accurately analyze the connection of steel plate and concrete through studs and the fracture of concrete, the steel plate is modeled by the shell element, the concrete is modeled by the solid element, and the stud is modeled by the spring element (axial spring and shear spring). Two models having different opening reinforcement shapes, circular and rectangular, are prepared. The material properties of concrete and steel plate are shown in Table 1 and Table 2. Table 3 shows the types of element and the constitutive law of materials. An analytical model is shown in Figure 13. The nonlinear finite element analysis program Abaqus / Standard (Dassault Systemes, ver. 2016 HF 4) is used.

Table 3 Element and constitutive law

Materials	Element	Constitutive law
Concrete	Solid element, size: approximately 24 mm	Isotropic damage plastic theory
Steel plate	Shell element, size: approximately 24 mm	Metal plastic theory
Stud	Spring element (axial and shear spring)	Multi-linear model

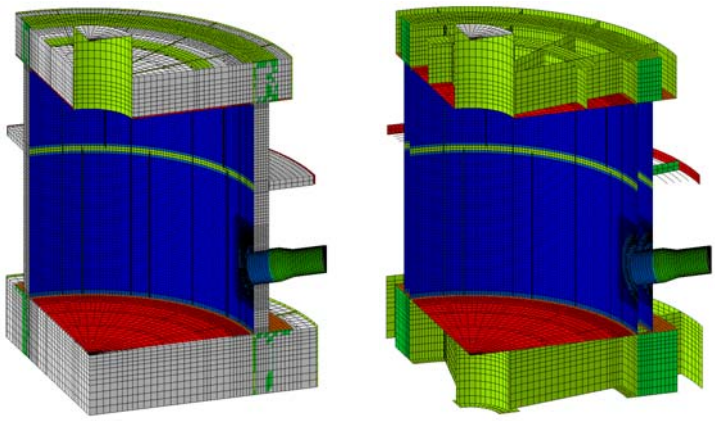

(a) Steel + Concrete (b) Steel only

Figure 13 Analytical model

ANALYTICAL RESULTS

As shown in Figure 14, the analytical results and the experimental results are in good agreement for the pressure-transverse deformation relationship. The differences in the transverse deformation of the circular opening reinforcement and the rectangular opening reinforcement are appropriately simulated. Figure 15 shows the vertical cross-section distribution of transverse deformation for 191.25° (around the opening) and 281.25° (rib position). Transverse deformation at each internal pressure level obtained by simulation analysis shows good agreement with experimental results throughout specimen heights. Figure 16 compares the maximum principal strain around the opening of the inner steel plate. In the experiment, strain of approximately 9,000 μ is confirmed by the circumferential force because of the internal pressure in the thick part just above the opening. The same degree of strain is also generated in the thick part near the opening in the analysis (① in the figure). The concentration of strain in the area where the thickness of the steel plate around the opening is switched almost agrees with the analysis and experiment (② in the figure). In addition, the vertical tensile strain due to bending at the base of the inner steel plate also shows good agreement between the analysis and the experiment (③ in the figure). The maximum principal strain contour of concrete is shown with pictures of the cutting surface of the specimen in Figure 17. A large tensile strain can be confirmed in the analysis at the position where the crack occurred, so the analytical results show good agreement with the experimental results.

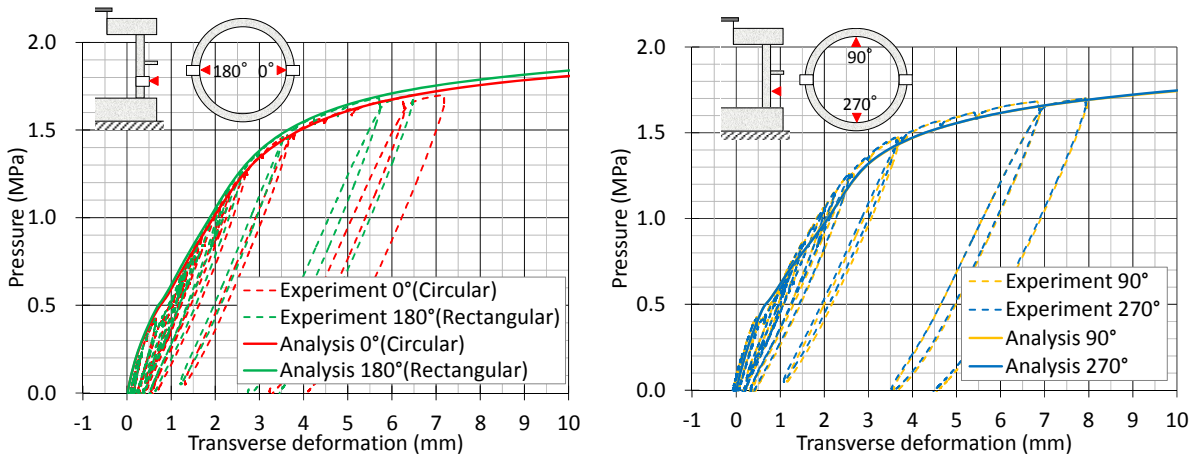

Figure 14 Comparison in pressure-transverse deformation relationship

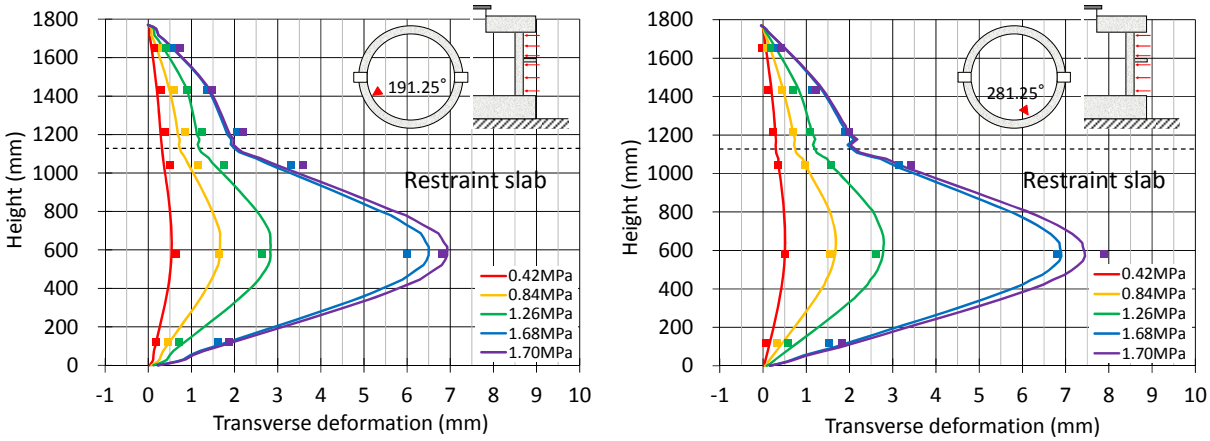

Figure 15 Comparison in vertical cross section distribution of transverse deformation

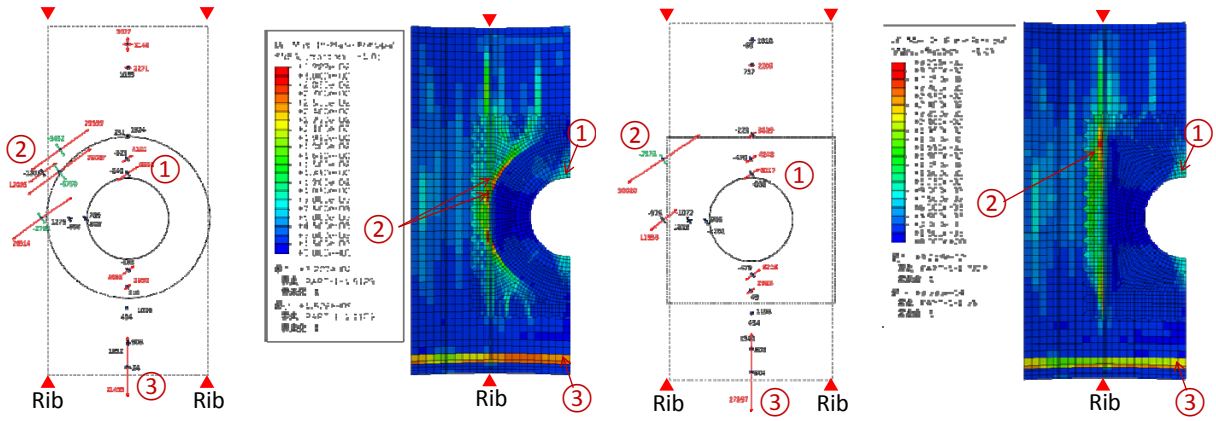

(a) 0° (Circular reinforcement) (b) 90° (Rectangular reinforcement)

Figure 16 Comparison in the maximum principal strain around the opening of the inner steel plate.

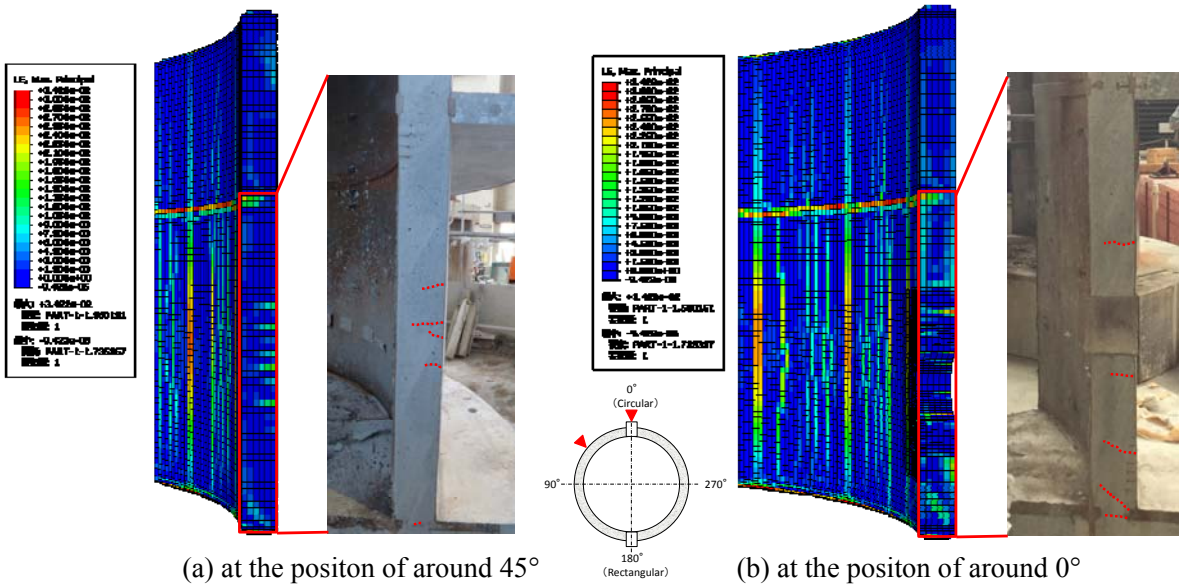

(a) at the positon of around 45° (b) at the positon of around 0°

Figure 17 Maximum principal strain contour of concrete with the cutting surface of the specimen

CONCLUSIONS

A pressure test with a cylindrical SC specimen having access tunnel openings and considering the constraining effect by the diaphragm floor and the peripheral floor was conducted in order to grasp the behavior of the SC structure shell wall against the pressure load. Judging from the state of the steel plate strain and the damage condition of the concrete, the final failure mode of this type of specimen may be bending failure due to the tensile fracture of the inner steel plate at the base. As a result of the comparative evaluation of the analytical results and experimental results, the analysis can adequately simulate the state of steel plate strain and the damage situation of the concrete in the experiment. From the above study, it is shown that the failure mode of the SCCV (shell wall) against an accident pressure load can be evaluated by the analytical method, which can evaluate the experiment with high accuracy.

ACKNOWLEDGEMENTS

This work was mainly carried out during FY 2011–2016 as the Japan national project “Development of Integrity Evaluation Method for PCV Structure” with the participation of the Chugoku Electric Power Company, Inc.; Tohoku Electric Power Company, Inc.; Tokyo Electric Power Company, Inc.; Chubu Electric Power Company, Inc.; Hokuriku Electric Power Company, Inc.; The Japan Atomic Power Company; Electric Power Development Company, Ltd.; the Institute of Applied Energy, Toshiba Corporation; and Hitachi-GE Nuclear Energy, Ltd. We would like to thank Dr. T. Nishikawa, professor emeritus at Tokyo Metropolitan University, Dr. K. Takiguchi, professor emeritus at Tokyo Institute of Technology, Dr. I. Maruyama, professor at Nagoya University, and Dr. Y. Kitsutaka, professor at Tokyo Metropolitan University for their valuable discussions.

REFERENCES

[1] Horschel, D.S., 1992, Experimental results from pressure testing a 1:6-scale nuclear power plant containment, NUREG/CR-5121 SAND88-0906,
[2] E, Saito et al., 1988, The development of Reinforced Concrete Containment Vessel (RCCV) (Part 4) Experiment of RCCV top slab – Experiment plan -, Summary of Technical Papers od Annual Meeting, Architectural Institute of japan, pp.1237-1238
[3] E, Saito et al., 1988, The development of Reinforced Concrete Containment Vessel (RCCV) (Part 5) Experiment of RCCV top slab – Test data and evaluation -, Summary of Technical Papers od Annual Meeting, Architectural Institute of japan, pp.1239-1240
[4] E, Saito et al., 1988, The development of Reinforced Concrete Containment Vessel (RCCV) (Part 6) Test on total model in large scale (1/6 scale) – Experimental plan -, Summary of Technical Papers od Annual Meeting, Architectural Institute of japan, pp.1241-1242
[5] E, Saito et al., 1988, The development of Reinforced Concrete Containment Vessel (RCCV) (Part 7) Test on total model in large scale (1/6 scale) – Inner pressure experiment -,Summary of Technical Papers od Annual Meeting, Architectural Institute of japan, pp.1243-1244
[6] Hessheimer, M.F., et al., 2001, Preliminary results of a 1:4-scale prestressed concrete containment vessel model test, Transactions, SMiRT16, Washington DC,
[7] The Japan Society Mechanical Engineers, 2008, Codes for Nuclear Power Generation Facilities – Rules on Design and Construction for Nuclear Power Plants -, JSME S NC1-2008
[8] Japanese Industrial Standards, 2016, JIS G3115, Steel plates for pressure vessels for intermediate temperature service
[9] Japanese Industrial Standards, 2002, JIS Z 2329, Methods for bubble leak testing